Original Article

MOLECULAR METABOLISM

ApoA-1 improves glucose tolerance by increasing glucose uptake into heart and skeletal muscle independently of AMPKα_2

Andreas Mæchel Fritzen [1], Joan Domingo-Espín [2], Anne-Marie Lundsgaard [1], Maximilian Kleinert [1,3], Ida Israelsen [1], Christian S. Carl [1], Trine S. Nicolaisen [1], Rasmus Kjøbsted [1], Jacob F. Jeppesen [4], Jørgen F.P. Wojtaszewski [1], Jens O. Lagerstedt [2,5,], Bente Kiens [1,*]**

ABSTRACT

Objective: Acute administration of the main protein component of high-density lipoprotein, apolipoprotein A-I (ApoA-1), improves glucose uptake in skeletal muscle. The molecular mechanisms mediating this are not known, but in muscle cell cultures, ApoA-1 failed to increase glucose uptake when infected with a dominant-negative AMP-activated protein kinase (AMPK) virus. We therefore investigated whether AMPK is necessary for ApoA-1-stimulated glucose uptake in intact heart and skeletal muscle *in vivo*.

Methods: The effect of injection with recombinant human ApoA-1 (rApoA-1) on glucose tolerance, glucose-stimulated insulin secretion, and glucose uptake into skeletal and heart muscle with and without block of insulin secretion by injection of epinephrine (0.1 mg/kg) and propranolol (5 mg/kg), were investigated in 8 weeks high-fat diet-fed (60E%) wild-type and AMPKα_2 kinase-dead mice in the overnight-fasted state. In addition, the effect of rApoA-1 on glucose uptake in isolated skeletal muscle ex vivo was studied.

Results: rApoA-1 lowered plasma glucose concentration by 1.7 mmol/l within 3 h (6.1 vs 4.4 mmol/l; $p < 0.001$). Three hours after rApoA-1 injection, glucose tolerance during a 40-min glucose tolerance test (GTT) was improved compared to control (area under the curve (AUC) reduced by 45%, $p < 0.001$). This was accompanied by an increased glucose clearance into skeletal (+110%; $p < 0.001$) and heart muscle (+100%; $p < 0.001$) and an increase in glucose-stimulated insulin secretion 20 min after glucose injection (+180%; $p < 0.001$). When insulin secretion was blocked during a GTT, rApoA-1 still enhanced glucose tolerance (AUC lowered by 20% compared to control; $p < 0.001$) and increased glucose clearance into skeletal (+50%; $p < 0.05$) and heart muscle (+270%; $p < 0.001$). These improvements occurred to a similar extent in both wild-type and AMPKα_2 kinase-dead mice and thus independently of AMPKα_2 activity in skeletal- and heart muscle. Interestingly, rApoA-1 failed to increase glucose uptake in isolated skeletal muscles *ex vivo*.

Conclusions: In conclusion, ApoA-1 stimulates *in vivo* glucose disposal into skeletal and heart muscle independently of AMPKα_2. The observation that ApoA-1 fails to increase glucose uptake in isolated muscle *ex vivo* suggests that additional systemic effects are required.

Keywords Apolipoprotein A-1 (ApoA-1); AMP-Activated protein kinase (AMPK); Glucose uptake; Skeletal muscle; Insulin; Metabolism

1. INTRODUCTION

The main protein component of high-density lipoproteins (HDL), apolipoprotein A-I (ApoA-1), is best known for its involvement in the reverse cholesterol transport pathway that reduces the atherosclerotic burden in the vascular wall [1]. However, ApoA-1 has also been found to have a glucose controlling function. In cross-sectional studies, type 2 diabetes in humans is characterized by decreased fasting levels of plasma ApoA-1 [2]. In addition, circulating ApoA-1 levels are found to be inversely associated with insulin resistance in human patients with impaired glucose tolerance and to be an independent risk factor for impaired glucose tolerance [3]. Conversely, endurance exercise training for 12 weeks led to 10% increased fasting levels of circulating ApoA-1 in sedentary men [4]. When human ApoA-1 (either purified from plasma or recombinant) was administered to cultured myotubes, glucose uptake was increased [5–8]. In ApoA-1 knock-out mice,

[1]Section of Molecular Physiology, Department of Nutrition, Exercise, and Sports, Faculty of Science, University of Copenhagen, Copenhagen, Denmark [2]Department of Experimental Medical Science, Lund University, S-221 84, Lund, Sweden [3]Institute for Diabetes and Obesity, Helmholtz Diabetes Center at Helmholtz Zentrum München, German Research Center for Environmental Health, Germany [4]Global Drug Discovery, Novo Nordisk Cambridge, MA, USA [5]Lund Institute of Advanced X-ray and Neutron Science (LINXS), Lund, Sweden

*Corresponding author. Section of Molecular Physiology, Department of Nutrition, Exercise, and Sports, August Krogh Building, 13 Universitetsparken, DK-2100, Copenhagen, Denmark. E-mail: bkiens@nexs.ku.dk (B. Kiens).

**Corresponding author. Department of Experimental Medical Science, Lund University, S-221 84, Lund, Sweden. E-mail: jens.lagerstedt@med.lu.se (J.O. Lagerstedt).

Received October 2, 2019 • Revision received January 3, 2020 • Accepted January 24, 2020 • Available online 4 March 2020

https://doi.org/10.1016/j.molmet.2020.01.013

Abbreviations

ABCA1	ATP-binding cassette transporter 1
ACC	acetyl-CoA carboxylase
AICAR	5-aminoimidazole-4-carboxamide ribonucleotide
AMPK	AMP-activated protein kinase
AMPK-DN	dominant negative AMPK
ApoA-1	apolipoprotein A-1
AUC	area under the curve
BCA	bicinchoninic acid
DG	deoxyglucose
DPM	disintegrations per minute
EDL	extensor digitorum longus
eNOS	endothelial nitric oxide synthase
ERK1/2	extracellular signal-regulated kinase 1/2
GLUT4	glucose transporter 4
GS	glycogen synthase
GSK3	glycogen synthase kinase 3
GTT	glucose tolerance test
HDL	high-density lipoprotein
HFD	high-fat diet
KD	kinase-dead
KRB	Krebs—Ringer buffer
MLV	multilamellar vesicles
PBS	phosphate-buffered saline
PCR	polymerase chain reaction
PET-CT	positron emission tomography-computed tomography
PVDF	polyvinylidene difluoride
rApoA-1	recombinant ApoA-1
rHDL	Reconstituted HDL
SDS-PAGE	sodium dodecyl sulfate—polyacrylamide gel electrophoresis
WT	wild-type

glucose tolerance was impaired [5,9] and insulin-stimulated glucose uptake in glycolytic muscles was lower than in wild-type (WT) controls [9], whereas overexpression of ApoA-1 in mice improved insulin tolerance [9,10]. Furthermore, treatment with ApoA-1 purified from human plasma for 2 or 4 weeks in obese mice improved glucose and insulin tolerance [11]. Similar findings have been reported in people with type 2 diabetes, in whom infusion of reconstituted HDL, consisting of ApoA-1 complexed with phosphatidylcholine, increased plasma insulin levels and reduced plasma glucose levels [6]. Torcetrapib, a small molecule inhibitor of cholesteryl ester transfer protein activity that increased plasma HDL cholesterol and ApoA-1 levels by approximately 70%, also improved glycemic control in humans with type 2 diabetes [12].

Recently, acute rApoA-1 administration to high-fat diet (HFD)-induced insulin-resistant mouse models led to improved glucose tolerance [13—16]. By using positron emission tomography (PET)-computed tomography (CT) and ^{18}F-labeled fluorodeoxyglucose, these effects appeared to relate to increases in skeletal muscle glucose uptake [14,15], partially due to ApoA-1 enhancement of glucose-stimulated insulin secretion [13,17,18]. However, rApoA-1 has also been suggested to stimulate glucose uptake into heart and skeletal muscle by insulin-independent mechanisms [8,14,15]. The molecular mechanisms mediating the increased insulin-independent glucose uptake into heart and skeletal muscle are not well described.

The heterotrimeric energy sensor AMP-activated protein kinase-complex (AMPK), consisting of a catalytic α-subunit (α_1 or α_2) in combination with regulatory β (β_1 or β_2) and γ-subunits (γ_1, γ_2 or γ_3), is a central regulator of the energy status of the cell and regulates a myriad of metabolic pathways [19—22]. On the basis of studies in cell cultures, it has been suggested that AMPK is activated by ApoA-1 and is of importance for ApoA-1-mediated glucose uptake in muscle. Thus, AMPK was shown to be activated by ApoA-1 (either purified from plasma or recombinant) in cultured rodent and human myocytes [5—7]. Moreover, in human skeletal muscle cell cultures from type 2 diabetic patients, the ApoA-1-stimulated glucose uptake was abolished when AMPK signaling was inhibited by an adenovirus-delivered dominant negative AMPK (AMPK-DN) mutant [6]. However, it is not known whether AMPK is of importance for ApoA-1-induced glucose uptake in mature striated muscle.

Pharmacological activation of AMPK by 5-aminoimidazole-4-carboxamide ribonucleotide (AICAR) is sufficient to increase glucose uptake into perfused heart [23] and isolated rodent skeletal muscle [24,25]. However, whether AMPK is activated by ApoA-1 and mediates ApoA-1-induced glucose uptake into heart and skeletal muscle *in vivo* in intact tissue is not known.

To examine whether the glucose metabolic improvements by ApoA-1 administration require muscle AMPKα_2 activity *in vivo*, we utilized a mouse model with muscle-specific over-expression of a kinase-dead α_2 AMPK subunit, which severely blunts AMPK activity in heart and skeletal muscle [26—28].

2. MATERIALS AND METHODS

2.1. Animals

Eight-to 10 week-old female C57Bl/6J mice (Janvier labs, France) and 8- to 10-week-old C57Bl/6 female mice overexpressing a muscle-specific, kinase-dead AMPKα_2 construct (AMPKα_2 KD) and corresponding WT littermates were used as previously described [26,27]. Briefly, the AMPKα_2 KD mice overexpress a kinase-inactive Lys45-to-Arg mutant of the AMPKα_2 protein, driven by a heart- and skeletal muscle-specific creatine kinase promoter. The transgenic AMPKα_2KD and corresponding WT mice were littermates from breeding of hemizygous transgenic mice and WT mice. Genotyping was performed by polymerase chain reaction (PCR) analysis on tail DNA using the following primers: endogenous AMPKα1 allele (CTG GCA GGT AGG CTC AGC AGG T, CTG CAA CCC TAT AGG TGG AAC AAC A) and AMPKα_2-KD transgene (CCC GGG GGA TCC ACT AGT TCT, CCA GCA CGT AGT GTC CGA TCT TC) and was later verified by immunoblotting. AMPKα_2 KD mice have nearly absent AMPKα_2 activity and more than 50% lower AMPKα_1 activity in skeletal muscle [28].

All mice were housed in temperature-controlled (22 $\pm$ 1 °C) facilities, maintained on a 12:12 h light—dark cycle with light turned on at 6.00 AM, and received standard chow (Altromin, cat. no. 1324; Brogaarden, Denmark) and water ad libitum. Eight weeks prior to the *in vivo* experiments and for some of the *ex vivo* incubation experiments, mice had ad libitum access to HFD comprising 60 E% fat (D12492, Research Diets, US). All experiments and the breeding protocol were approved by the Danish Animal Experimental Inspectorate and complied with the European Convention for the Protection of Vertebrate Animals Used for Experiments and Other Scientific Purposes (ETS No. 123).

2.2. Design

The role of AMPK in rApoA-1-induced muscle glucose uptake was evaluated both in an *in vivo* experiment with injection of rApoA-1 in 8-weeks HFD-fed WT and AMPKα_2 KD mice. In addition, the role of

rApoA-1 in isolated muscle *ex vivo* was evaluated by incubation with rApoA-1 in chow-fed C57Bl/6 mice (*ex vivo* experiments 1 and 2) and in 8-weeks HFD-fed WT and AMPKα_2 KD mice (*ex vivo* experiment 3).

2.3. Expression and purification of recombinant human ApoA-1

Human recombinant ApoA-1 (rApoA-1) containing a His-tag at the N-terminus was expressed in *Escherichia coli* bacteria and purified using immobilized metal affinity chromatography followed by tobacco etch virus protease treatment to remove the His-tag, as previously described [29–31].

2.4. Reconstituted HDL preparation

Reconstituted HDL (rHDL) particles were prepared as previously described [32]. In brief, lyophilized DMPC (1,2-dimyristoyl-sn-glycero-3-phosphocholine; Avanti Polar Lipids, Alabaster, AL, USA) was dissolved in 3:1 chloroform:methanol solution. The solvent was completely evaporated by overnight incubation under a stream of nitrogen gas. DMPC was then dissolved in phosphate-buffered saline (PBS), and the lipid suspension was extruded through a 100-nm polycarbonate membrane using the LiposoFast system (Avestin, Ottawa, ON, Canada) to form multilamellar vesicles (MLV). rHDL was produced by incubating the recombinant protein with MLVs at a protein to lipid molar ratio of 1:100 at 24 °C, the transition temperature for DMPC, for 96 h.

2.5. In vivo experiment; glucose tolerance test and glucose-induced glucose clearance

Mice fasted overnight (12 h) were injected intraperitoneally with either rApoA-1 (14 mg/kg in isotonic saline, pH 7.4) or saline as control (vehicle). Glucose (2 g/kg BW) was injected intraperitoneally 3 h after rApoA-1 treatments. ^{3}H-2-deoxyglucose (2-DG) (0.6 μCi/g BW) was co-administered with the glucose to allow for measurement of tissue-specific glucose-induced glucose clearance, and epinephrine at 0.1 mg/kg (catalog #E4250, Sigma–Aldrich, Denmark) and propranolol at 5 mg/kg (catalog #P0884; Sigma–Aldrich, Denmark) were co-administered with the glucose where indicated, as in [14,33,34], to block pancreatic insulin secretion. For blood glucose measurements, mixed tail blood was obtained at 0, 10, 20, 30, and 40 min after glucose and analyzed with a glucometer (Contour XT, Bayer, CH). At 20 min, blood was collected into capillary tubes. Plasma insulin concentration was measured by enzyme-linked immunosorbent assay (ELISA, Mouse Insulin ELISA, Alpco, US). At 40 min, mice were sacrificed by cervical decapitation, trunk blood was collected, and tissues were quickly excised (tibialis anterior and gastrocnemius muscles, heart, and liver) and snap-frozen in liquid nitrogen.

2.6. Ex vivo muscle incubations

Muscle incubations were performed as previously described [24]. In brief, non-fasted mice were anesthetized by intraperitoneal injection of pentobarbital (10 mg/100 g BW) before soleus and extensor digitorum longus (EDL) muscles were dissected and suspended in incubation chambers (Multi Wire Myograph System; DMT, Denmark) containing Krebs–Ringer buffer (KRB) (117 mmol/L NaCl, 4.7 mmol/L KCl, 2.5 mmol/L $CaCl_2$, 1.2 mmol/L KH_2PO_4, 1.2 mmol/L $MgSO_4$, 0.5 mmol/L $NaHCO_3$, pH 7.4) supplemented with 0.1% bovine serum albumin (BSA), 8 mmol/L mannitol, and 2 mmol/L pyruvate. During the incubation, the buffer was oxygenated with 95% O_2 and 5% CO_2 and maintained at 30 °C. After 10 min of preincubation, paired muscles from each animal were incubated for 30 min (experiment 1) or 3 h (experiments 2 and 3) in the absence or presence of lipid-free (experiments 1 and 2) or lipidated (experiment 3) rApoA-1 (rHDL) at varying doses (0–400 μg/ml in experiment 1, 60 μg/ml in experiment 2–3). As positive controls, muscles were incubated for 30 min in KRB in the presence of a maximal concentration (10,000 μU/mL) of insulin (Actrapid; Novo Nordisk, Bagsvaerd, Denmark) or 2 mmol/L 5-aminoimidazole-4-carboxamide ribonucleotide (AICAR) (Toronto Research Chemicals, Canada). The uptake of ^{3}H-2-DG was measured during the last 10 min by adding 1 mmol/L ^{3}H-2-DG (0.056 MBq/mL) and 7 mmol/L ^{14}C-mannitol (0.0167 MBq/mL) to the incubation medium. After incubation, muscles were harvested, washed in ice-cold KRB, quickly dried on paper, and frozen in liquid nitrogen.

2.7. Tissue processing

Tissues were pulverized in liquid nitrogen using a mortar and pestle. Then, 25 mg of skeletal and heart muscle or the entire mass of EDL and soleus muscles from the incubation experiments were homogenized in ice-cold buffer as previously described [27] for 2 × 60 s at 30 Hz using steel beads and a TissueLyzer II (QIAGEN, Germany). Homogenates were rotated end-over-end for 1 h before centrifugation at 16,000 g for 20 min. The supernatant (lysate) was collected, frozen in liquid nitrogen, and stored at −80 °C for later analyses.

2.8. In vivo glucose-induced glucose clearance

Plasma ^{3}H activity was measured in 5 μl of plasma by scintillation counting (Ultima Gold and Tri-Carb 2910 TR; PerkinElmer, US) at 20 and 40 min, and the average plasma ^{3}H-2-DG exposure was estimated. Twenty to 30 mg of each tissue was used to determine the accumulation of phosphorylated ^{3}H-2-DG (^{3}H-2-DG-6-P) by the precipitation method [35]. Glucose clearance was calculated by dividing tissue ^{3}H-2-DG-6-P disintegrations per minute (DPM), accumulated in tissue over 40 min from tracer injection, by average ^{3}H-2-DG DPM in blood sampled during this period [36].

2.9. Ex vivo glucose uptake

Glucose uptake in the incubation experiments was assessed by the accumulation of ^{3}H-2-DG in muscle with the use of ^{14}C-mannitol (PerkinElmer, MA, US) as an extracellular marker. Radioactivity was measured in 250 μL of lysate by liquid scintillation counting (Ultima Gold and Tri-Carb 2910 TR; PerkinElmer, MA, US) and related to the specific activity of the incubation buffer.

2.10. Glycogen

Liver glycogen concentration was determined in 5 mg of pulverized tissue after acidic hydrolysis and measured spectrophotometrically at 340 nm (Hitachi 912 Automatic Analyzer; Boehringer, DE).

2.11. Western blotting

Protein content and phosphorylation levels were determined in muscle lysates as previously described [37]. In brief, total protein concentration of muscle lysates was determined in triplicate using the bicinchoninic acid (BCA) method with a Pierce BCA protein assay (no. 23227; Pierce Biotechnology, IL, US). A maximal coefficient of variance of 5% was accepted between replicates. All samples were heated (96 °C in 5 min) in Laemmli buffer before being subjected to sodium dodecyl sulfate–polyacrylamide gel electrophoresis (SDS-PAGE) and semi-dry immunoblotting. The primary antibodies used are shown in Table S1. Membranes were probed with enhanced chemiluminescence (ECL$^+$; Amersham Biosciences, NJ, USA), and immune complexes were visualized using a BioRad ChemiDoc MP Imaging System (CA, US). Signals were quantified (Image Lab version 4.0, BioRad, CA, US) and presented relative to the WT vehicle group without insulin block within the given experiment. Loading consistencies and similar total protein

content in samples were verified by Coomassie staining. Coomassie staining after development was performed by submersion of polyvinylidene difluoride (PVDF) membranes for 10 min in 0.5% Coomassie Blue G-250 in 50% ethanol/10% acetic acid, removal of excess Coomassie-stain with distilled water followed by destaining in 50% ethanol/10% acetic acid until bands were clearly visible.

2.12. Statistics

All data are expressed as means ± SEM. The statistical analyses performed are described in each figure legend. Statistical significance was defined as $p < 0.05$. Statistical analyses were performed in GraphPad PRISM 8 (GraphPad, CA, US).

3. RESULTS

In the *in vivo* experiment, body weight was not different between WT and AMPKα_2 KD mice when initiating the experiments after 8 weeks of HFD feeding (Figure S1). After an overnight fast, WT and AMPKα_2 KD mice were injected with rApoA-1 as illustrated in Figure 1A. Within 3 h, rApoA-1 lowered the blood glucose concentration by 1.7 mmol/l ($p < 0.001$) in both WT and AMPKα_2 KD mice compared with saline-treated control mice (Figure 1B). A GTT performed 3 h after rApoA-1 injection revealed that glucose tolerance, assessed as area under the curve (AUC) of the blood glucose curves during the GTT, was improved by 45% ($p < 0.001$) by rApoA-1 in both WT and AMPKα_2 KD mice compared with saline-treated control mice (Figure 1C—D). This was associated with an increased glucose-stimulated plasma insulin concentration (+180%; $p < 0.001$) after 20 min in rApoA-1-treated mice compared with controls (Figure 1E). To isolate the role of ApoA-1 on tissues from the effect of improved glucose-stimulated insulin secretion, rApoA-1- and saline-treated WT and AMPKα_2 KD mice were also co-administered with an insulin blockade at the start of the GTT. This efficiently blocked the ApoA-1-induced increase in plasma insulin concentration at 20 min (Figure 1E; $p < 0.001$),

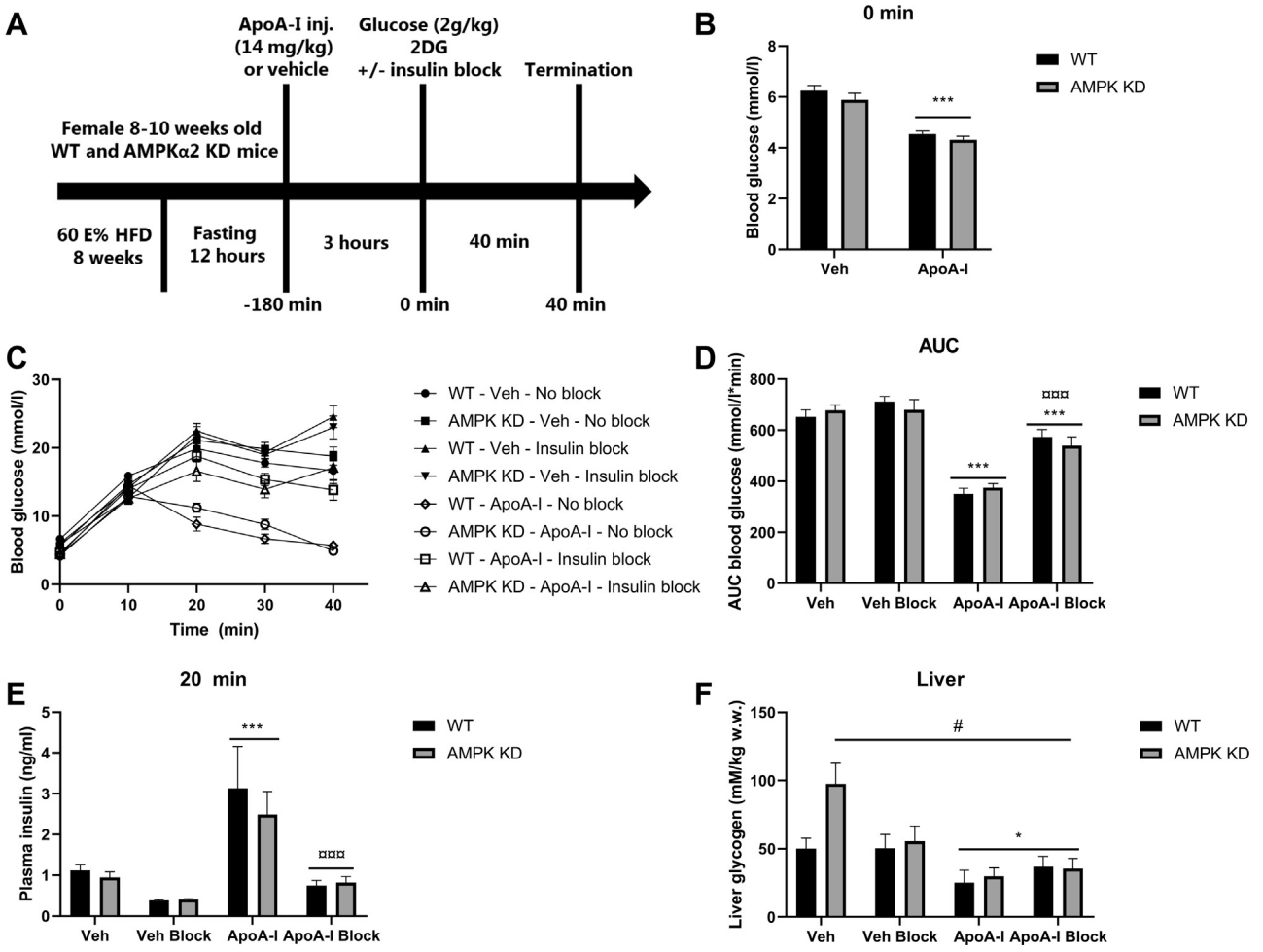

Figure 1: Apolipoprotein A-I (ApoA-1) lowers fasting blood glucose and improves glucose tolerance by insulin-dependent and -independent mechanisms independently of muscle AMPKα_2. A, Experimental setup; 8- to 10-week-old wild-type (WT) and AMPKα_2 kinase-dead (KD) mice were high-fat diet (HFD)-fed for 8 weeks and then fasted overnight for 12 h. On the experimental day, WT and AMPKα_2 KD mice were intraperitoneally injected with either human recombinant ApoA-1 (14 mg/kg) or saline (NaCl; Veh). Three hours later, saline- and ApoA-1-treated WT and AMPKα_2 KD mice received ^{3}H-2-deoxyglucose (2DG) and glucose (2 g/kg BW) and were randomized to also receive insulin block containing epinephrine (0.1 mg/kg) and propranolol (5 mg/kg) or Veh. Blood glucose concentrations at 0 min (B), time-course (C), and area under the curve (AUC; D) for the subsequent 40 min glucose tolerance test (GTT), plasma insulin concentrations at 20 min (E), and liver glycogen content at 40 min (F). Data are presented as means ± SEM. n = 11—13 collected from 2 independent experiments. Three-way ANOVAs were applied in B—F. * Main effect ($p < 0.05$) of ApoA-1 independently of genotype and insulin block. *** Main effect ($p < 0.001$) (within insulin blockade/no blockade in D and E). ¤¤¤ Main effect ($p < 0.001$) of insulin block within ApoA-1 independently of genotype. # Main effect ($p < 0.05$) of genotype independently of ApoA-1 and insulin block.

although slightly higher, but not statistically significant, plasma insulin levels were observed in the insulin-blocked situation after rApoA-1 compared to the saline-treated control mice (Figure 1E). In this insulin blocked situation, glucose tolerance was still improved by 20% ($p < 0.001$) by ApoA-1 treatment in both WT and AMPKα_2 KD mice compared with saline-treated control mice (Figure 1C—D). Despite the blood glucose lowering effects of rApoA-1, liver glycogen contents following the GTT were lowered on average 43% ($p < 0.05$) by rApoA-1 in both WT and AMPKα_2 KD mice compared with saline-treated control mice, independently of insulin blockade (Figure 1F), implying that the lower glycemia during the GTT by rApoA-1 were related to increased peripheral glucose disposal rather than decreased hepatic output. To investigate this further, glucose-stimulated glucose clearance was traced into skeletal and heart muscle. Mimicking the improvements in whole-body glucose tolerance, rApoA-1 treatment increased glucose-stimulated glucose clearance into skeletal (Figure 2A—B) and heart muscle (Figure 2C) by 110% and 100% ($p < 0.001$), respectively. Even with insulin blockade, rApoA-1 increased glucose clearance by 50% in skeletal (Figure 2A—B; $p < 0.05$) and 270% in heart muscle (Figure 2C; $p < 0.001$). Importantly, improvements in glucose clearance were evident to the same extent in WT and AMPKα_2 KD mice and thus independent of AMPKα_2 activity in skeletal and heart muscle (Figure 2A—C).

3.1. AMPK signaling

A similar enhancement in muscle glucose clearance by rApoA-1 in WT and AMPKα_2 KD mice was consistent with the lack of increase in AMPK signaling with rApoA-1 administration in skeletal (Figure 3A—B and D-E) and heart muscle (Figure 3C,F), judged by unchanged phosphorylation of AMPK (Figure 3A—C) and the downstream target, acetyl-CoA carboxylase (ACC) (Figure 3D—F) in WT mice. As expected, due to the overexpression of a dominant negative AMPKα_2 construct, both AMPKα_2 protein and phosphorylation of AMPK at Thr172 (Figure S2) were increased in the skeletal and heart muscle of AMPKα_2 KD compared with the WT mice. However, when phosphorylation was related to total protein, AMPK Thr172 phosphorylation was unaffected (Figure 3A—C). Phosphorylation of ACC (indicative of AMPK activity) was decreased in AMPKα_2 KD mice compared to WT ($p < 0.01$; Figure 3D—F) independently of any changes in ACC1 protein content.

3.2. Akt, ERK, and GS signaling

To investigate whether enhanced proximal insulin signaling could account for the rApoA-1-induced glucose clearance into skeletal and heart muscle, Akt phosphorylation at Ser473 and Thr308 was assessed in tissues taken at 40 min of the GTT. rApoA-1 treatment induced 32% higher ($p < 0.05$) Akt Ser473 phosphorylation and 28% higher ($p < 0.05$) Akt Thr308 phosphorylation in the tibialis anterior muscles of WT and AMPKα_2 KD mice independently of the insulin blockade (Figure 4A). However, this effect of rApoA-I was not observed in gastrocnemius (Figure 4B and E) or heart muscle (Figure 4C and F), although 2-way analysis of variance (ANOVA) within the insulin-blocked groups revealed a tendency for rApoA-1 to increase Akt Ser473 and Thr308 phosphorylation in heart muscle (50%; $p = 0.08$) but not in gastrocnemius muscle (25%; $p = 0.2$). Akt phosphorylation at Ser473 and at Thr308 were decreased ($p < 0.01$) with the insulin blockade in both skeletal (Figure 4A-B+4D-E) and heart muscle (Figure 4C and F) of both WT and AMPKα_2 KD mice compared with mice not treated with insulin blockade. These changes were not driven by changes in total protein content, since Akt2 protein content was not affected by rApoA-1, insulin blockade, or genotype.

Phosphorylation of extracellular signal-regulated kinase 1/2 (ERK1/2) at Thr202/Tyr204 was not affected by either rApoA-1 treatment, insulin blockade, or genotype in skeletal and heart muscle (Figure 4G—I).

To evaluate whether an increased covalently-regulated glycogen synthesis contributed to the increased glucose clearance in skeletal and heart muscle, phosphorylation of glycogen synthase (GS) at site 3a + b was investigated. In skeletal muscle, phosphorylation of the inhibitory site 3a + b at GS were not affected by rApoA-1 treatment, insulin blockade, or genotype (Figure 5A—B). In contrast, in the hearts of both WT and AMPK KD mice, GS phosphorylation at site 3a + b was 85% and 185% increased ($p < 0.001$) with rApoA-1 treatment compared to vehicle in the non-blocked and insulin-blocked conditions, respectively. Also, GS phosphorylation at site 3a + b in the heart was lower ($p < 0.001$) in AMPK KD compared to WT mice (Figure 5C). These changes were not driven by changes in total protein content, since GS protein content was not affected by rApoA-1, insulin blockade, or genotype.

The upstream kinase of GS, the glycogen synthase kinase 3 (GSK3) protein, was similarly regulated. GSK3α Ser21 phosphorylation was not affected by rApoA-1 treatment in skeletal muscle (Figure 5D—E), whereas GSK3α Ser21 phosphorylation increased ($p < 0.05$) in the hearts of both WT and AMPK KD mice with rApoA-1 treatment compared to vehicle in the non-blocked and insulin-blocked conditions, respectively (Figure 5F). Also, GSK3α Ser21 phosphorylation was lowered by the insulin blockade in tibialis anterior (Figure 5D) and heart (Figure 5F), but not in gastrocnemius (Figure 5E). These changes were

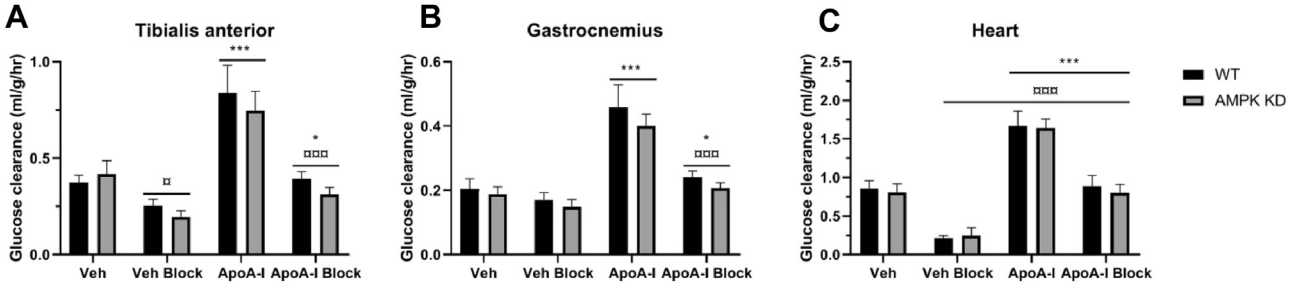

Figure 2: Apolipoprotein A-I (ApoA-1) increases glucose clearance into skeletal muscle and heart by insulin-dependent and -independent mechanisms independently of muscle AMPKα_2. Glucose-stimulated glucose clearance into tibialis anterior (A), gastrocnemius (B), and heart (C) in wild-type (WT) and AMPKα_2 kinase-dead (KD) high-fat diet (HFD)-fed mice treated with ApoA-1 (14 mg/kg) or saline (Veh) and with or without insulin blockade (0.1 mg/kg epinephrine and 5 mg/kg propranolol). Data are presented as means ± SEM. n = 11—13. Three-way ANOVAs were applied in A-C. * Main effect ($p < 0.05$) of ApoA-1 within insulin blockade independently of genotype. *** Main effect ($p < 0.001$) of ApoA-1 independently of genotype (within no insulin blockade in A and B). ¤/¤¤¤ Main effect ($p < 0.05$/$p < 0.001$) of insulin blockade independently of genotype (within insulin blockade in A and B). Hr, hour.

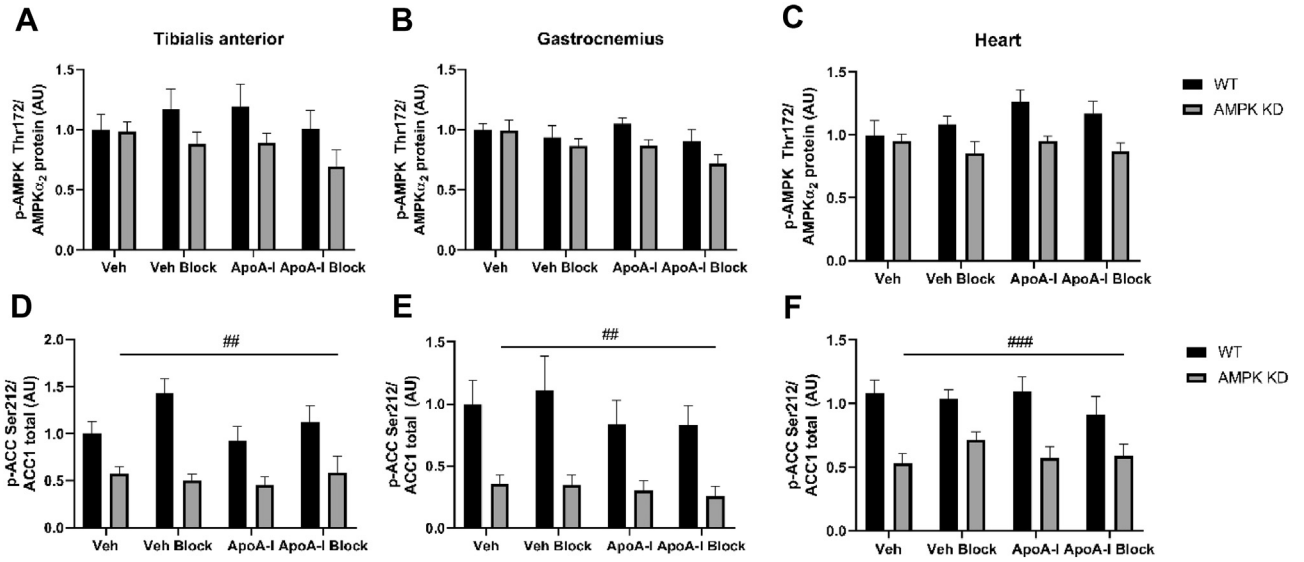

Figure 3: Apolipoprotein A-I (ApoA-1) does not affect AMPK signaling in skeletal muscle and heart. Phosphorylation of AMP-activated protein kinase (AMPK) at Thr172/ AMPKα_2 protein (A—C) and acetyl-CoA carboxylase (ACC) at Ser212/ACC1 protein (D—F) in tibialis anterior (A and D), gastrocnemius (B and E) and heart (C and F) of wild-type (WT) and AMPKα_2 kinase-dead (KD) high-fat diet (HFD)-fed mice treated with ApoA-1 (14 mg/kg) or saline (Veh) and with or without insulin blockade (0.1 mg/kg of epinephrine and 5 mg/kg of propranolol). Representative blots are shown in Fig. S2. Data are presented as means ± SEM. n = 11—13. Three-way ANOVAs were applied in A-F. ##/### Main effect ($p < 0.01/p < 0.001$) of genotype independently of ApoA-1 and insulin blockade. AU, arbitrary units.

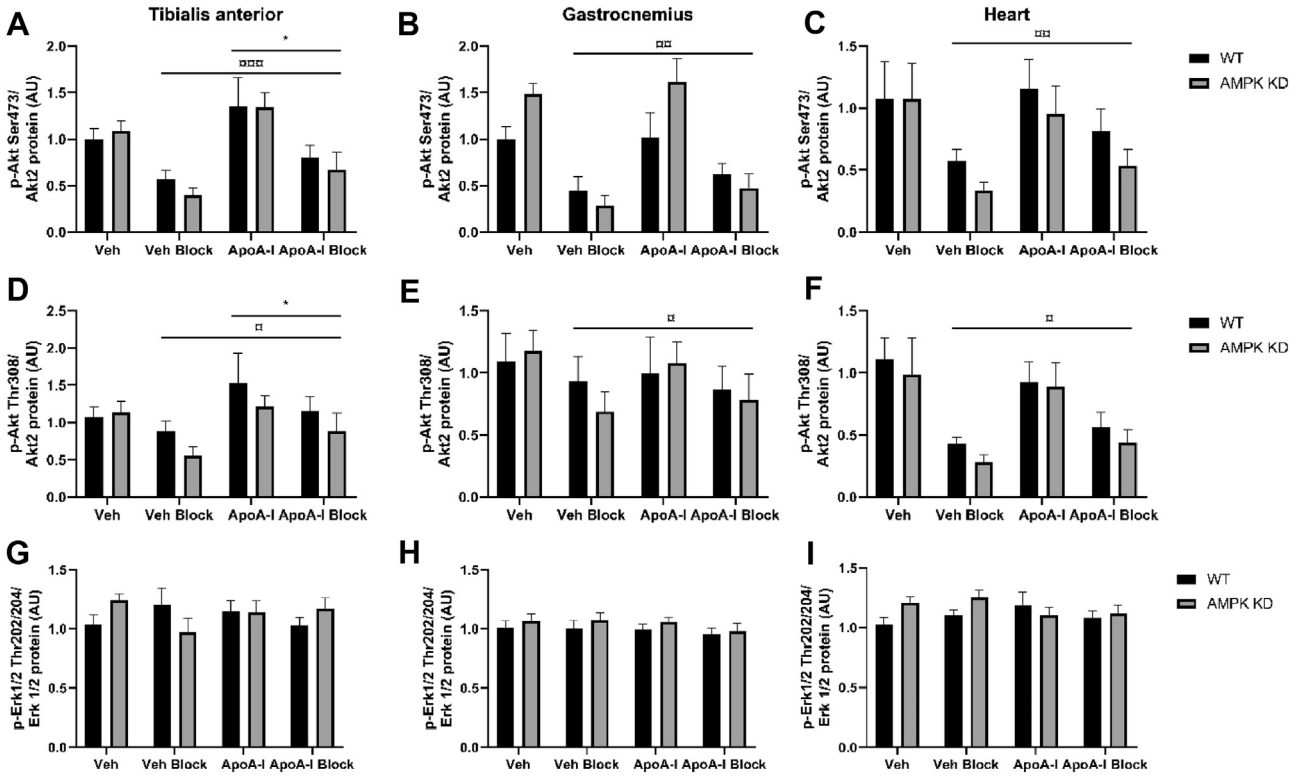

Figure 4: Apolipoprotein A-I (ApoA-1) affects Akt phosphorylation in skeletal muscle. Phosphorylation of Akt at Ser473 (A—C) and at Thr308 (D—F) as well as extracellular signal—regulated kinases (ERK)1/2 at Thr202/204 (G—I) in tibialis anterior (A, D and G), gastrocnemius (B, E and H), and heart (C, F and I) of wild-type (WT) and AMPKα_2 kinase-dead (KD) high-fat diet (HFD)-fed mice treated with ApoA-1 (14 mg/kg) or saline (Veh) and with or without insulin blockade (0.1 mg/kg of epinephrine and 5 mg/kg of propranolol). Representative blots are shown in Fig. S2. Data are presented as means ± SEM. n = 11—13. Three-way ANOVAs were applied in A-I. ¤¤/¤¤¤ Main effect ($p < 0.01/p < 0.001$) of insulin blockade independently of ApoA-1 and genotype. */*** Main effect ($p < 0.05/p < 0.001$) of ApoA-1 independently of insulin blockade and genotype. ### Main effect ($p < 0.001$) of genotype independently of insulin blockade and genotype. AU, arbitrary units.

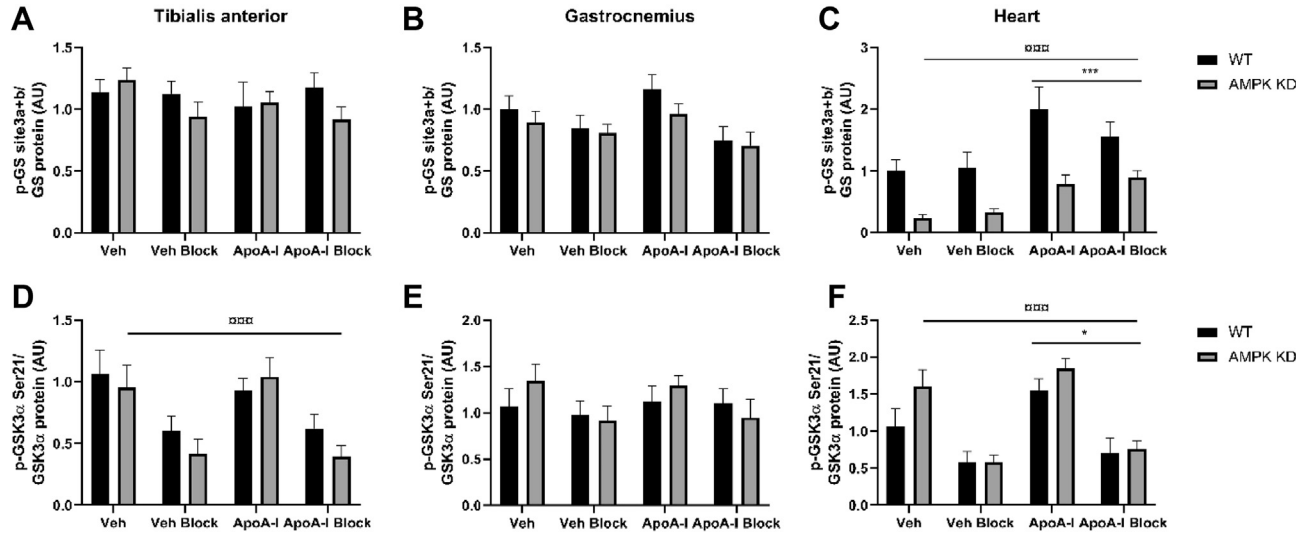

Figure 5: Apolipoprotein A-I (ApoA-1) affects GS phosphorylation in heart. Phosphorylation of glycogen synthase (GS) at site 3a + b (A–C) and GSK3α at Ser21 (D–F) in tibialis anterior (A and D), gastrocnemius (B and E), and heart (C and F) of wild-type (WT) and AMPKα_2 kinase-dead (KD) high-fat diet (HFD)-fed mice treated with ApoA-1 (14 mg/kg) or saline (Veh) and with or without insulin blockade (0.1 mg/kg of epinephrine and 5 mg/kg of propranolol). Representative blots are shown in Fig. S2. Data are presented as means ± SEM. n = 11–13. Three-way ANOVAs were applied in A-F. ¤¤¤ Main effect ($p < 0.01$/$p < 0.001$) of insulin blockade independently of ApoA-1 and genotype. */*** Main effect ($p < 0.05$/$p < 0.001$) of ApoA-1 independently of insulin blockade and genotype. AU, arbitrary units.

not driven by changes in total protein content, since GSK3α protein content was not affected by rApoA-1, insulin blockade, or genotype.

3.3. Ex vivo muscle incubations

Incubation with various doses of lipid-free rApoA-1 (4–400 μg/ml) for 30 min increased glucose uptake in neither isolated glycolytic EDL (Figure 6A) nor oxidative soleus muscle (Figure 6B). In previous studies, using muscle cell cultures [6–8,15,38] or isolated murine muscle [5], incubation with rApoA-1 lasted for a period of 10–120 min. To verify that 30 min incubation duration was insufficient to exert an effect on glucose uptake, we next incubated EDL and soleus muscles with lipid-free rApoA-1 (60 μg/ml) or vehicle for 3 h as in the *in vivo* experiment. However, rApoA-1 incubation for 3 h increased glucose uptake in neither EDL (Figure 6C) nor soleus muscles (Figure 6D). Because rApoA-1 is reported to be fully lipidated in the circulation 3 h after intraperitoneal injection in mice and to have formed lipid–protein complexes [13,30], we incubated EDL and soleus muscles with lipidated rApoA-1 (reconstituted HDL) for 3 h to determine whether the lipidation level of the rApoA-1 was responsible for the observed divergent effects on muscle glucose uptake between *in vivo* and *ex vivo* incubation conditions. However, lipidated ApoA-1 (60 μg/ml) did not affect glucose uptake in isolated skeletal muscles *ex vivo* (Figure 6E–F). Furthermore, AMPK signaling, evaluated by the phosphorylation of the AMPK and the downstream target, ACC, was not affected by rApoA-1 (Figure 6G-J + S2B). Collectively, these findings show that rApoA-1 treatment does not increase glucose uptake during *ex vivo* conditions in incubated glycolytic or oxidative skeletal muscle, which indicates the need for a systemic factor or a regulatory role for perfusion of the mouse skeletal muscle for the rApoA-1-induced insulin-independent glucose clearance observed *in vivo*.

4. DISCUSSION

Here, we show that rApoA-1 administration lowered fasting blood glucose and improved glucose tolerance in HFD-fed mice. This was mainly driven by rApoA-1 increasing the glucose-stimulated insulin secretion, in congruence with previous findings [13,14,17,18], emphasizing that rApoA-1 treatment primes the β-cells to be more responsive to a glucose load. This confirms *ex vivo* findings in β-cells, in which ApoA-1 has been shown to induce both insulin secretion and synthesis [16,17,39]. At the same time, we also show that rApoA-1 improved glucose tolerance and increased glucose clearance into skeletal and heart muscle *in vivo* when insulin secretion was blocked. Importantly, the effects of rApoA-1 on glucose tolerance or skeletal and heart muscle glucose clearance were not found to be reliant on AMPKα_2 in either the non-blocked or insulin-blocked conditions. In agreement, AMPK signaling was not activated by rApoA-1 administration in skeletal and heart muscle *in vivo* or in isolated muscles *ex vivo*. This suggests that other molecular mechanisms than AMPK signaling are responsible for ApoA-1 action on glucose clearance in skeletal and heart muscle *in vivo* in mice and highlights the importance of verifying evidence from cell culture studies in intact tissue *in vivo*.

We found that rApoA-1 under glucose-stimulated conditions induced a minor increase in Akt phosphorylation in tibialis anterior muscle and a trend to the same in the heart in the insulin-blocked situation, but not in the gastrocnemius muscle. This is consistent with the findings that ApoA-1 overexpression in mice only led to higher basal Akt phosphorylation and insulin-stimulated glucose uptake in glycolytic muscles like tibialis anterior and EDL, but not in more oxidative muscles, such as soleus and gastrocnemius [9]. Thus, in the present study, rApoA-1-induced Akt signaling may contribute to the observed effects of rApoA-1 on *in vivo* glucose clearance, at least in the glycolytic muscles. However, this regulation seems not to be the entire mechanism, especially since we observed increased glucose clearance in the gastrocnemius muscle without changes in Akt signaling. The lack of a consistent increase in Akt phosphorylation across all tissues in the insulin-blocked conditions with rApoA-1 compared to the saline-treated mice also support that the non-significantly higher plasma insulin levels in this situation seem not to be a potent contributing mechanism to the rApoA-1-induced improvement in glucose tolerance and heart and skeletal muscle glucose uptake.

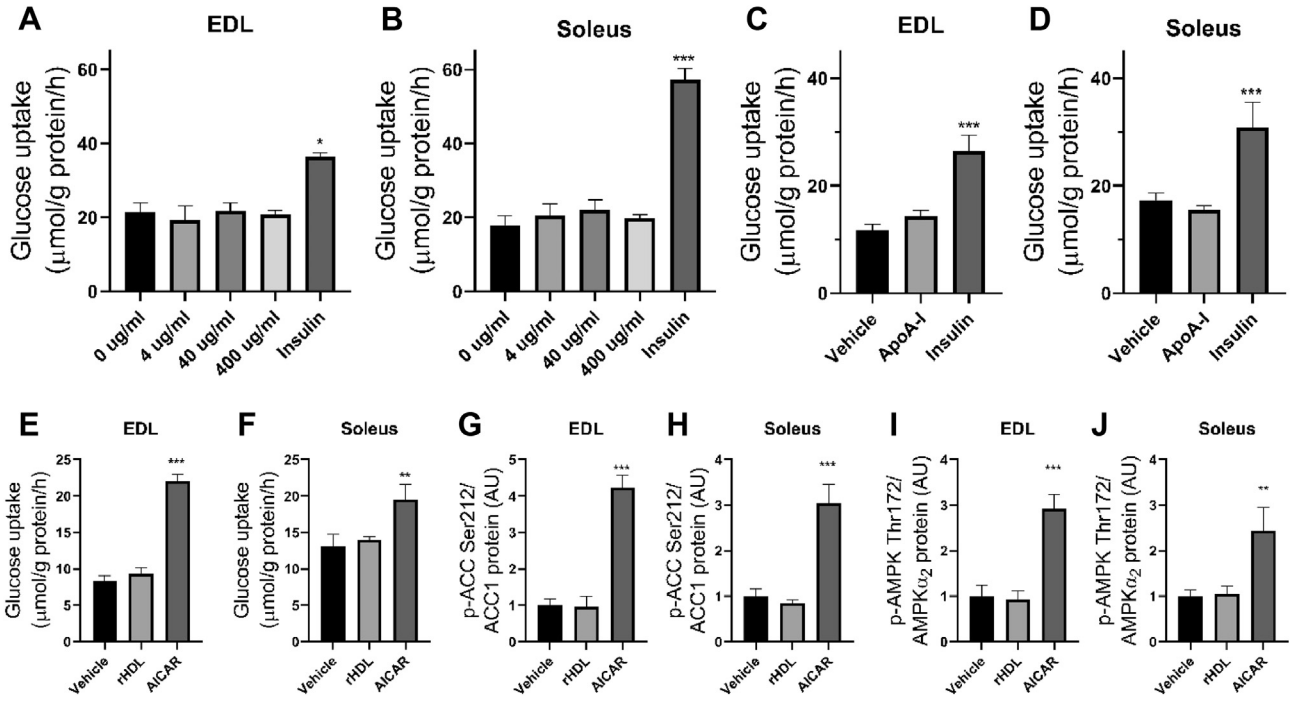

Figure 6: Apolipoprotein A-I (ApoA-1) does not stimulate glucose uptake or AMPK signaling in isolated skeletal muscle. A-B, Glucose uptake in isolated extensor digitorum longus (EDL; A) and soleus (B) of chow-fed C57Bl/6J female mice in response to varying doses of lipid-free ApoA-1 (0—400 μg/ml) incubated for 30 min and insulin (10,000 μU/ml) as control. C-D, Glucose uptake in isolated extensor digitorum longus (EDL; C) and soleus (D) of 8-week high-fat diet (HFD)-fed C57Bl/6J female mice in response to incubation with lipid-free ApoA-1 for 3 h (60 μg/ml) and vehicle and insulin (10,000 μU/ml) as controls. E-H, Glucose uptake (E—F) and phosphorylation of acetyl-CoA carboxylase (ACC) at Ser212/ACC1 protein (G—H) and phosphorylation of AMP-activated protein kinase (AMPK) at Thr172/AMPKα_2 protein (I—J) in isolated extensor digitorum longus (EDL; E, G, and I) and soleus (F, H, and J) of 8-week HFD-fed C57Bl/6J female mice in response to *ex vivo* incubation with lipidated ApoA-1 (60 μg/ml) (rHDL) for 3 h and vehicle and the AMPK activator 5-Aminoimidazole-4-carboxamide ribonucleotide (AICAR; 2 mM) as controls. Data are presented as means ± SEM. n = 4—6 in A-B (n = 2 in insulin control). n = 8 in C-D (n = 4 in insulin control). n = 6 in E-J (n = 4 in AICAR WT). One-way ANOVAs were applied in A-D. 2-way ANOVAs were applied in E-J. */**/*** Significantly different ($p < 0.05/0.01/0.001$) from 0 μg/ml or vehicle. AU, arbitrary units.

To evaluate whether non-oxidative glucose disposal contributed to the increased clearance of plasma glucose, the inhibitory phosphorylation of GS at site 3a + b, which is suggested to play an important role in the regulation of GS activity [40], was examined. It was found that the phosphorylation of GS at site 3a + b and the upstream kinase GSK3α at Ser21 increased by rApoA-1 in the heart indicative of decreased GS activity after rApoA-1 treatment. In skeletal muscle, even though Akt phosphorylation was induced in tibialis anterior muscle, GS and GSK3 phosphorylations were not affected by rApoA-1 in either tibialis anterior and gastrocnemius muscle. This is in line with the findings of unchanged phosphorylation of the upstream kinase of GS, GSK3, in rApoA-1-treated skeletal muscle from obese mice [14] and unchanged skeletal muscle glycogen levels in both ApoA-1 knock-out mice and mice overexpressing ApoA-1 compared with WT [9]. These data indicate that the increased glucose clearance into either skeletal or heart muscle after rApoA-1 treatment is not due to a covalent regulation on GS.

In *ex vivo* incubated isolated skeletal muscle fibers, treatment with a subregion (190—243) of rApoA-1 was previously found to induce glucose transporter 4 (GLUT4) translocation [7], which could suggest that increased GLUT4-mediated glucose transport across the plasma membrane of the myocyte contributes to the rApoA-1-induced glucose uptake. However, we found here that full-length rApoA-1 incubation of isolated skeletal muscle *ex vivo* lacking the systemic and vascular *in vivo* conditions did not affect glucose uptake. This implies that a systemic factor or vascular properties related to the delivery of glucose or insulin to the muscle cells could be involved in mediating the rApoA-1-induced glucose clearance. In L6 myocytes, ApoA-1 induced insulin-stimulated glucose uptake without any increase in GLUT4 translocation [15], indicating that ApoA-1 improves glucose uptake independently of the glucose transport step *in vivo*. In support of a regulatory role of ApoA-1 in the perfusion of the skeletal muscle or in the endothelial transport of insulin and glucose, rApoA-1-induced glucose uptake in skeletal muscle was found to be associated with improved transport of glucose from arterial plasma to the intracellular space of the muscle using kinetic modeling of 18F-fludeoxyglucose transport in db/db mice [15]. Moreover, HDL particles have previously been shown to mediate increased production of the vasodilator endothelial nitric oxide synthase (eNOS) [41]. rApoA-1 was specifically shown to stimulate eNOS activity by direct protein association allowing multisite phosphorylation changes in endothelial cells [42]. A systemic mechanism of ApoA-I to increase glucose uptake is further supported by the notion that rApoA-1 increased glucose uptake into isolated skeletal muscle when rApoA-1 was injected *in vivo* in mice and thus initiated systemic effects for 2 h before mice were euthanized and gastrocnemius was removed and incubated [15]. Thus, it is plausible that rApoA-1-induced glucose uptake in muscle also relies on systemic mechanisms in addition to intrinsic, myocellular mechanisms associated with GLUT4-translocation, such as Akt signaling. A systemic-related mechanism challenges previous studies in cultured myotubes showing that administration of human ApoA-1 (either purified from plasma or recombinant) increased glucose uptake [5—8] without any systemic conditions. Effects of ApoA-1 in cultured myocytes could either indicate that some signaling components or metabolic regulatory mechanisms

are differentially affected by ApoA-1 in cell systems and in isolated intact skeletal muscles *ex vivo*. Alternatively, in addition to potential systemic regulatory effects of ApoA-1 on muscle glucose uptake, ApoA-1 may affect glucose uptake via other mechanisms, such as increased hexokinase activity [15], or via ATP-binding cassette transporter 1 (ABCA1)-mediated enhanced insulin signaling for glucose uptake [8] as previously suggested. Future studies are needed to further elaborate on the dependency and relative importance of systemic regulatory steps vs. myocyte intrinsic mechanisms for the increase in muscle glucose uptake mediated by ApoA-I *in vivo*. Also, incubation of muscles *ex vivo* with serum could be of interest to investigate whether a serum factor is of importance, as seen for insulin-stimulated muscle glucose uptake after *ex vivo* contractions [43]. However, serum was not used and thus not necessary for ApoA-1-mediated glucose uptake in cultured myocytes [5–8], in insulin-stimulated glucose uptake after pharmacological AMPK activation in isolated muscle *ex vivo* [44], or in isolated skeletal muscle glucose uptake measured *ex vivo* 2 h after injection of rApoA-1 *in vivo* [15].

To minimize stress from handling the mice, we chose to study female mice. Previous studies in male mice have found that rApoA-1 induced greater glucometabolic improvements in obese and glucose intolerant mice fed HFD for 2 weeks compared to lean mice fed a chow diet. In female mice in our animal facilities, 2 weeks of a similar HFD was not sufficient to induce substantial weight gain and glucose intolerance, so 8-week HFD-fed mice were investigated. This could be explained by findings suggesting that female mice gain weight slower than male mice [45,46] and that large metabolic variations are observed in mice from different housing institutions [47]. Together, previous studies and the present study show that rApoA-1 improves glucose tolerance and muscle glucose uptake independently of the gender of the mice.

Considering the glucose lowering properties of ApoA-1 concomitant with the beneficial effects on cholesterol efflux and the cardiovascular system, ApoA-1 mimetics have been suggested as a new anti-diabetic candidate [16]. Collectively, our data showing independency of AMPK for ApoA-1-induced glucometabolic effects provides opportunities for future research into whether combinatorial treatment of diabetes with ApoA-1 mimetics and AMPK activators [48–51] have enhanced efficacy, since they function through different signaling pathways.

In conclusion, we report that rApoA-1 lowers blood glucose and improves glucose tolerance in HFD-fed mice by increasing glucose disposal into skeletal and heart muscle, both with and without inhibition of circulating insulin. These effects are independent of muscle AMPKα_2, which was previously suggested in cell-based studies. Instead, we hypothesize that the vascular system or systemic factors are necessary for ApoA-1 to increase glucose uptake into muscle, because ApoA-1 was not able to induce glucose uptake in isolated muscle *ex vivo*.

AUTHOR CONTRIBUTIONS

A.M.F., J.D.-E., J.F.J., J.O.L., and B.K. conceptualized the study and planned and designed the experiments. A.M.F., J.D.-E., A.M.L., M.K. I.I., C.S.C., T.S.N., R.K., and J.F.P.W. performed the experiments and researched and analyzed data. A.M.F. and B.K. wrote the manuscript with all co-authors revising it critically for important intellectual content. All authors approved the final version of the manuscript.

ACKNOWLEDGMENTS

The authors acknowledge the skilled technical assistance of Irene Bech Nielsen, Betina Bolmgren, and Nicoline Resen Andersen (University of Copenhagen). We thank Professor Grahame Hardie at the University of Dundee for kindly providing antibodies. A.M.F, A-M.L., and R.K. were supported by a postdoctoral research grant from the Danish Diabetes Academy, funded by the Novo Nordisk Foundation (grant: NNF17SA0031406). A.M.F. was furthermore supported by the Benzon Foundation. M.K. is supported by a postdoctoral research grant from the Danish Council for Independent Research/Medicine (grant: 4004-00233). B.K. was funded by The University of Copenhagen Excellence Program for Interdisciplinary Research (2016): "Physical activity and Nutrition for Improvement of Health" and the Danish Council for independent Research/Medicine (grant: 4183-00249). J.O.L. was funded by the Swedish Research Council (K2014-54X-22426-01-3, 2016–02124 and 2009-1039, Strategic research area Exodiab), the Swedish Diabetes Foundation, the Albert Påhlsson Foundation, the Novo Nordisk Foundation, NovoNordisk A/S, the Krapperup Foundation, and by the Swedish Foundation for Strategic Research (IRC15-0067). J.D.E. was funded by the Diabetes Research and Wellness Foundation Sweden.

CONFLICT OF INTEREST

J.O.L. has filed for a patent (WO 2014/114787 A1) pertaining to the data described here. The authors declare that they have no other competing interests.

APPENDIX A. SUPPLEMENTARY DATA

Supplementary data to this article can be found online at https://doi.org/10.1016/j.molmet.2020.01.013.

REFERENCES

[1] Heinecke, J.W., 2012. The not-so-simple HDL story: a new era for quantifying HDL and cardiovascular risk? Nature Medicine 18(9):1346–1347.

[2] Drew, B.G., Rye, K.A., Duffy, S.J., Barter, P., Kingwell, B.A., 2012. The emerging role of HDL in glucose metabolism. Nature Reviews Endocrinology 8: 237–245.

[3] Feng, X., Gao, X., Yao, Z., Xu, Y., 2017. Low apoA-I is associated with insulin resistance in patients with impaired glucose tolerance: a cross-sectional study. Lipids in Health and Disease 16:69–446.

[4] Kiens, B., Jorgensen, I., Lewis, S., Jensen, G., Lithell, H., Vessby, B., et al., 1980. Increased plasma HDL-cholesterol and apo A-1 in sedentary middle-aged men after physical conditioning. European Journal of Clinical Investigation 10:203–209.

[5] Han, R., Lai, R., Ding, Q., Wang, Z., Luo, X., Zhang, Y., et al., 2007. Apolipoprotein A-I stimulates AMP-activated protein kinase and improves glucose metabolism. Diabetologia 50:1960–1968.

[6] Drew, B.G., Duffy, S.J., Formosa, M.F., Natoli, A.K., Henstridge, D.C., Penfold, S.A., et al., 2009. High-density lipoprotein modulates glucose metabolism in patients with type 2 diabetes mellitus. Circulation 119:2103–2111.

[7] Dalla-Riva, J., Stenkula, K.G., Petrlova, J., Lagerstedt, J.O., 2013. Discoidal HDL and apoA-I-derived peptides improve glucose uptake in skeletal muscle. The Journal of Lipid Research 54:1275–1282.

[8] Tang, S., Tabet, F., Cochran, B.J., Cuesta Torres, L.F., Wu, B.J., Barter, P.J., et al., 2019. Apolipoprotein A-I enhances insulin-dependent and insulin-independent glucose uptake by skeletal muscle. Scientific Reports 9:1350–38014.

[9] Lehti, M., Donelan, E., Abplanalp, W., Al-Massadi, O., Habegger, K.M., Weber, J., et al., 2013. High-density lipoprotein maintains skeletal muscle function by modulating cellular respiration in mice. Circulation 128:2364–2371.

[10] Ruan, X., Li, Z., Zhang, Y., Yang, L., Pan, Y., Wang, Z., et al., 2011. Apolipoprotein A-I possesses an anti-obesity effect associated with increase of energy expenditure and up-regulation of UCP1 in brown fat. Journal of Cellular and Molecular Medicine 15:763–772.

[11] McGrath, K.C., Li, X.H., Whitworth, P.T., Kasz, R., Tan, J.T., McLennan, S.V., et al., 2014. High density lipoproteins improve insulin sensitivity in high-fat diet-fed mice by suppressing hepatic inflammation. The Journal of Lipid Research 55:421—430.

[12] Barter, P.J., Rye, K.A., Tardif, J.C., Waters, D.D., Boekholdt, S.M., Breazna, A., et al., 2011. Effect of torcetrapib on glucose, insulin, and hemoglobin A1c in subjects in the investigation of lipid level management to understand its impact in atherosclerotic events (ILLUMINATE) trial. Circulation 124:555—562.

[13] Stenkula, K.G., Lindahl, M., Petrlova, J., Dalla-Riva, J., Goransson, O., Cushman, S.W., et al., 2014. Single injections of apoA-I acutely improve in vivo glucose tolerance in insulin-resistant mice. Diabetologia 57:797—800.

[14] Domingo-Espin, J., Lindahl, M., Nilsson-Wolanin, O., Cushman, S.W., Stenkula, K.G., Lagerstedt, J.O., 2016. Dual actions of apolipoprotein A-I on glucose-stimulated insulin secretion and insulin-independent peripheral tissue glucose uptake lead to increased heart and skeletal muscle glucose disposal. Diabetes 65:1838—1848.

[15] Cochran, B.J., Ryder, W.J., Parmar, A., Tang, S., Reilhac, A., Arthur, A., et al., 2016. In vivo PET imaging with [(18)F]FDG to explain improved glucose uptake in an apolipoprotein A-I treated mouse model of diabetes. Diabetologia 59: 1977—1984.

[16] Edmunds, S.J., Liebana-Garcia, R., Nilsson, O., Domingo-Espin, J., Gronberg, C., Stenkula, K.G., et al., 2019. ApoAI-derived peptide increases glucose tolerance and prevents formation of atherosclerosis in mice. Diabetologia 4877.

[17] Cochran, B.J., Bisoendial, R.J., Hou, L., Glaros, E.N., Rossy, J., Thomas, S.R., et al., 2014. Apolipoprotein A-I increases insulin secretion and production from pancreatic beta-cells via a G-protein-cAMP-PKA-FoxO1-dependent mechanism. Arteriosclerosis, Thrombosis, and Vascular Biology 34:2261—2267.

[18] Rye, K.A., Barter, P.J., Cochran, B.J., 2016. Apolipoprotein A-I interactions with insulin secretion and production. Current Opinion in Lipidology 27:8—13.

[19] Kjobsted, R., Hingst, J.R., Fentz, J., Foretz, M., Sanz, M.N., Pehmoller, C., et al., 2018. AMPK in skeletal muscle function and metabolism. The FASEB Journal 32:1741—1777.

[20] Hoffman, N.J., Parker, B.L., Chaudhuri, R., Fisher-Wellman, K.H., Kleinert, M., Humphrey, S.J., et al., 2015. Global phosphoproteomic analysis of human skeletal muscle reveals a network of exercise-regulated kinases and AMPK substrates. Cell Metabolism 22:922—935.

[21] Schaffer, B.E., Levin, R.S., Hertz, N.T., Maures, T.J., Schoof, M.L., Hollstein, P.E., et al., 2015. Identification of AMPK phosphorylation sites reveals a network of proteins involved in cell invasion and facilitates large-scale substrate prediction. Cell Metabolism 22:907—921.

[22] Steinberg, G.R., Kemp, B.E., 2009. AMPK in Health and disease. Physiological Reviews 89(3):1025—1078.

[23] Russell III, R.R., Bergeron, R., Shulman, G.I., Young, L.H., 1999. Translocation of myocardial GLUT-4 and increased glucose uptake through activation of AMPK by AICAR. American Journal of Physiology 277:H643—H649.

[24] Kjobsted, R., Treebak, J.T., Fentz, J., Lantier, L., Viollet, B., Birk, J.B., et al., 2015. Prior AICAR stimulation increases insulin sensitivity in mouse skeletal muscle in an AMPK-dependent manner. Diabetes 64(6):2042—2055.

[25] Merrill, G.F., Kurth, E.J., Hardie, D.G., Winder, W.W., 1997. AICA riboside increases AMP-activated protein kinase, fatty acid oxidation, and glucose uptake in rat muscle. American Journal of Physiology 273(6 Pt 1):E1107—E1112.

[26] Mu, J., Brozinick Jr., J.T., Valladares, O., Bucan, M., Birnbaum, M.J., 2001. A role for AMP-activated protein kinase in contraction- and hypoxia-regulated glucose transport in skeletal muscle. Molecular Cell 7(5):1085—1094.

[27] Fritzen, A.M., Frosig, C., Jeppesen, J., Jensen, T.E., Lundsgaard, A.M., Serup, A.K., et al., 2016. Role of AMPK in regulation of LC3 lipidation as a marker of autophagy in skeletal muscle. Cellular Signalling 28:663—674.

[28] Jensen, T.E., Schjerling, P., Viollet, B., Wojtaszewski, J.F., Richter, E.A., 2008. AMPK alpha1 activation is required for stimulation of glucose uptake by twitch contraction, but not by H2O2, in mouse skeletal muscle. PloS One 3(5):e2102.

[29] Petrlova, J., Duong, T., Cochran, M.C., Axelsson, A., Morgelin, M., Roberts, L.M., et al., 2012. The fibrillogenic L178H variant of apolipoprotein A-I forms helical fibrils. The Journal of Lipid Research 53:390—398.

[30] Petrlova, J., Dalla-Riva, J., Morgelin, M., Lindahl, M., Krupinska, E., Stenkula, K.G., et al., 2014. Secondary structure changes in ApoA-I Milano (R173C) are not accompanied by a decrease in protein stability or solubility. PloS One 9:e96150.

[31] Del, G.R., Lagerstedt, J.O., 2018. High-efficient bacterial production of human ApoA-I amyloidogenic variants. Protein Science 27:2101—2109.

[32] Del, G.R., Domingo-Espin, J., Iacobucci, I., Nilsson, O., Monti, M., Monti, D.M., et al., 2017. Structural determinants in ApoA-I amyloidogenic variants explain improved cholesterol metabolism despite low HDL levels. Biochimica et Biophysica Acta - Molecular Basis of Disease 1863:3038—3048.

[33] Shen, S.W., Reaven, G.M., Farquhar, J.W., 1970. Comparison of impedance to insulin-mediated glucose uptake in normal subjects and in subjects with latent diabetes. Journal of Clinical Investigation 49:2151—2160.

[34] Taketomi, S., Ikeda, H., Ishikawa, E., Iwatsuka, H., 1982. Determination of overall insulin sensitivity in diabetic mice. KK. Hormone and Metabolic Research 14:14—18.

[35] Ferre, P., Leturque, A., Burnol, A.F., Penicaud, L., Girard, J., 1985. A method to quantify glucose utilization in vivo in skeletal muscle and white adipose tissue of the anaesthetized rat. Biochemical Journal 228:103—110.

[36] Fazakerley, D.J., Fritzen, A.M., Nelson, M.E., Thorius, I.H., Cooke, K.C., Humphrey, S.J., et al., 2019. Insulin tolerance test under anaesthesia to measure tissue-specific insulin-stimulated glucose disposal. Bio-protocol 9: e3146.

[37] Fritzen, A.M., Madsen, A.B., Kleinert, M., Treebak, J.T., Lundsgaard, A.M., Jensen, T.E., et al., 2015. Regulation of autophagy in human skeletal muscle - effects of exercise, exercise training and insulin stimulation. The Journal of Physiology.

[38] Zhang, Q., Zhang, Y., Feng, H., Guo, R., Jin, L., Wan, R., et al., 2011. High density lipoprotein (HDL) promotes glucose uptake in adipocytes and glycogen synthesis in muscle cells. PloS One 6:e23556.

[39] Fryirs, M.A., Barter, P.J., Appavoo, M., Tuch, B.E., Tabet, F., Heather, A.K., et al., 2010. Effects of high-density lipoproteins on pancreatic beta-cell insulin secretion. Arteriosclerosis, Thrombosis, and Vascular Biology 30:1642—1648.

[40] Skurat, A.V., Roach, P.J., 1995. Phosphorylation of sites 3a and 3b (Ser640 and Ser644) in the control of rabbit muscle glycogen synthase. Journal of Biological Chemistry 270:12491—12497.

[41] Yuhanna, I.S., Zhu, Y., Cox, B.E., Hahner, L.D., Osborne-Lawrence, S., Lu, P., et al., 2001. High-density lipoprotein binding to scavenger receptor-BI activates endothelial nitric oxide synthase. Nature Medicine 7:853—857.

[42] Drew, B.G., Fidge, N.H., Gallon-Beaumier, G., Kemp, B.E., Kingwell, B.A., 2004. High-density lipoprotein and apolipoprotein AI increase endothelial NO synthase activity by protein association and multisite phosphorylation. Proceedings of the National Academy of Sciences of the U S A 101:6999—7004.

[43] Gao, J., Gulve, E.A., Holloszy, J.O., 1994. Contraction-induced increase in muscle insulin sensitivity: requirement for a serum factor. American Journal of Physiology 266:E186—E192.

[44] Jorgensen, N.O., Wojtaszewski, J.F.P., Kjobsted, R., 2018. Serum is not necessary for prior pharmacological activation of AMPK to increase insulin sensitivity of mouse skeletal muscle. International Journal of Molecular Sciences 19:ijms19041201.

[45] Pettersson, U.S., Walden, T.B., Carlsson, P.O., Jansson, L., Phillipson, M., 2012. Female mice are protected against high-fat diet induced metabolic syndrome and increase the regulatory T cell population in adipose tissue. PloS One 7:e46057.

[46] Yang, Y., Smith Jr., D.L., Keating, K.D., Allison, D.B., Nagy, T.R., 2014. Variations in body weight, food intake and body composition after long-term high-fat diet feeding in C57BL/6J mice. Obesity 22:2147—2155.

[47] Corrigan, J.K., Ramachandran, D., He, Y., Palmer, C., Jurczak, M.J., Li, B., et al., 2019. A big-data approach to understanding metabolic rate and response to obesity in laboratory mice bioRxiv839076.

[48] Hawley, S.A., Fullerton, M.D., Ross, F.A., Schertzer, J.D., Chevtzoff, C., Walker, K.J., et al., 2012. The ancient drug salicylate directly activates AMP-activated protein kinase. Science 336(6083):918—922.

[49] Fullerton, M.D., Galic, S., Marcinko, K., Sikkema, S., Pulinilkunnil, T., Chen, Z.P., et al., 2013. Single phosphorylation sites in Acc1 and Acc2 regulate lipid homeostasis and the insulin-sensitizing effects of metformin. Nature Medicine 19:1649—1654.

[50] Cokorinos, E.C., Delmore, J., Reyes, A.R., Albuquerque, B., Kjobsted, R., Jorgensen, N.O., et al., 2017. Activation of skeletal muscle AMPK promotes glucose disposal and glucose lowering in non-human primates and mice. Cell Metabolism 25:1147—1159.

[51] Steinberg, G.R., Carling, D., 2019. AMP-activated protein kinase: the current landscape for drug development. Nature Reviews Drug Discovery, 10-0019.

